

Hole transport in organic field-effect transistors with active poly(3-hexylthiophene) layer containing CdSe quantum dots

U. BIELECKA^{1,3*}, P. LUTSYK^{1,2}, M. NYK¹, K. JANUS¹, M. SAMOC¹, W. BARTKOWIAK^{1†},
S. NESPUREK³

¹Institute of Physical and Theoretical Chemistry, Chemistry Department, Wrocław University of Technology,
Wyspińskiego 27, 50-370 Wrocław, Poland

²Institute of Physics, National Academy of Science of Ukraine, prospekt Nauky 46, 03680 Kyiv, Ukraine

³Institute of Macromolecular Chemistry AS CR, Heyrovsky Sq. 2, 162 06 Prague 6, Czech Republic

Hybrid field-effect transistors (FETs) based on poly(3-hexylthiophene) (P3HT) containing CdSe quantum dots (QDs) were fabricated. The effect of the concentration of QDs on charge transport in the hybrid material was studied. The influence of the QDs capping ligand on charge transport parameters was investigated by replacing the conventional trioctylphosphine oxide (TOPO) surfactant with pyridine to provide closer contact between the organic and inorganic components. Electrical parameters of FETs with an active layer made of P3HT:CdSe QDs blend were determined, showing field-effect hole mobilities up to $1.1 \times 10^{-4} \text{ cm}^2/\text{Vs}$. Incorporation of TOPO covered CdSe QDs decreased the charge carrier mobility while the pyridine covered CdSe QDs did not alter this transport parameter significantly.

Keywords: *organic field effect transistor; quantum dots; poly(3-hexylthiophene); hybrid material*

© Wrocław University of Technology.

1. Introduction

Organic field effect transistors (OFETs) have attracted much attention over last 20 years [1–4] and, as a part of the progress in their design and fabrication, OFET devices based on hybrid materials have also been extensively studied [3–5]. Semiconductor nanoparticles (NPs) embedded into a matrix, most commonly a polymeric one, are an example of modern engineered hybrid material systems. Among various wide band-gap materials useful for NP fabrication and incorporation into the matrices, cadmium selenide (n-type semiconductor) is interesting due to size-dependent emission and simple, two-step protocol of synthesis [6]. These systems are known to possess unique optoelectrical and photonic properties useful e.g. for photovoltaic systems, but, up to date, the mechanism of charge carrier transport in the hybrid

materials has not been extensively described in the literature. Investigations of transport phenomena in nanocomposites evoked some controversy and the results were contradictory [3–5].

Usually, QDs are capped with a layer, which is essential for avoiding a broad size distribution, and protects QDs from aggregation during storage. The role of the ligand and the surface modification through ligand exchange has been vigorously discussed [7–9] and was tested in the case of pyridine, butyl amine or alkylthiols which were used to replace TOPO or oleic acid [10]. Such modification, using e.g. pyridine, minimizes the distance between QDs and the matrix, which modifies the electrochemical properties and interaction of QDs with the surroundings [11–13]. Recently, P3HT:pyridine-CdSe QDs composite was investigated as a donor-acceptor system suitable for organic-based solar cells [14]. The formation of grains and radiative recombination of photogenerated excitons were investigated in the blend with the mass ratio of P3HT:CdSe QDs equal

*E-mail: urszula.bielecka@pwr.wroc.pl

†E-mail: wojciech.bartkowiak@pwr.wroc.pl

to 1:8. The decisive factor limiting the photovoltaic efficiency seemed to be the morphology of the blend. Replacing TOPO by pyridine via solution exchange method was presented in [15], where the problem of solubility and its influence on the efficiency of fabricated device was discussed. Optimization of the annealing, thermal decomposition and reduction processes also influenced the morphology and properties of QDs increasing the power conversion efficiency of QD layer from 0.02 % for as-synthesized CdSe QDs to 0.05 % for nitrogen-annealed CdSe QDs [16].

Minimizing the distance between the organic (P3HT) and inorganic (CdSe QD) components and uniform dispersion of QDs amplified the electronic interactions resulting in faster fluorescence decay and changes in the emission spectra as well as charge and energy transfer properties [17].

Charge carrier transport in organic-inorganic systems was investigated by various methods. For instance, time-of-flight experiments performed on QDs embedded into a polymer (PVK) matrix, showed an enhancement of the effective charge carrier mobility [18]. On the other hand, the studies of OFETs with a metallic nanoparticle layer between the active and dielectric layer showed a reduction of the charge carrier mobility. It is probable that charge carriers became localized on metal dots, which resulted in physical disorder at the insulator/semiconductor interface. It was suggested that nanoparticles acted as trapping centers [19]. Other studies demonstrated that gold nanoparticles in Au/P3HT blends had no influence on the transport properties of the polymer matrix [20].

It was established that incorporation of ZnO nanocrystals into poly[2-methoxy-5-(2'-ethylhexyloxy)-p-phenylene vinylene] (MEH-PPV) polymer matrix, increased the hole mobility by up to three orders of magnitude [21]. Because of high energy barrier between the polymer and inorganic component, it was impossible for a hole to be transferred from organic to inorganic component. ZnO acted then as an "anti-trapping" center. The explanation of the enhancement of mobility by the anti-trapping centers seemed to be the most probable, however, no ligand effect

was discussed. Aldakov et al. [8] showed that the insulating character of the ligand influenced the energy diagram, which was the basis of the mechanism proposed by Xu et al. [21]. In thin film transistors ZnO sometimes forms large size grains at the insulator/semiconductor interface which results in decreasing the density of defects in the active layer. Consequently, the density of interface states at the grain boundaries is reduced and the electronic properties are improved [22, 23]. Despite the huge progress in FETs/OFETs technology, only a few papers have described the optical and electrical properties of hybrid FET systems with semiconductor QDs [24].

The problem of pyridine as an insulating capping surface of the QDs in the active layer of OFETs has been discussed in literature [24]. It has been reported that weakly bound pyridine can be removed from the surface of a nanoparticle in vacuum and pyridine capped CdSe QDs are poorly soluble in chloroform based P3HT solutions. It is suspected that positive charge carriers from the polymer recombine with the electrons released from QDs which results in source-drain current decay. In the same article the charge carrier mobility was found to be slightly enhanced by addition of CdSe QDs to the P3HT polymer (50 % enhancement, dark current).

The aim of this work is to follow the results presented in refs [10–12, 14] by studying the electrical properties of blends obtained by physical mixing of CdSe QDs and P3HT. To understand the influence of the QDs capping ligand on charge transport parameters the conventional TOPO is replaced by smaller pyridine; the distance between the organic and inorganic component can thus be minimized. Electrical parameters of organic field effect transistors with active layers made of P3HT:CdSe blends are analyzed.

2. Experimental

2.1. QDs synthesis

The synthesis of CdSe QDs followed a protocol similar to that described recently by Nyk et al. [25]. In a typical synthesis the selenium

precursor was made by mixing 0.4 g of selenium powder (95 %, Sigma Aldrich) and 10 g of TOP (trioctylphosphine, Sigma Aldrich) in a dry box under inert atmosphere. Additionally, 20 g of TOPO (90 % trioctylphosphine oxide, Sigma Aldrich) and 0.25 g of cadmium acetate (Sigma Aldrich) were added to a three-necked flask. The cadmium salt was heated to 110 °C under vacuum with stirring for about 30 min. To remove water and oxygen, the flask was purged with dry nitrogen at 10 min intervals. The transparent solution was then heated to 330 °C under nitrogen and vigorous stirring. At this temperature the selenium stock solution was swiftly injected into the reaction vessel in a single step. The reaction was stopped 1.5 min after the injection by removing the heating mantle and cooling to room temperature. The mixture was precipitated with methanol in an ultrasonic bath and collected by centrifugation at 14000 rpm for 30 min. The precipitate was dried in vacuum and dispersed in 5 ml anhydrous chloroform. The above mentioned procedure was applied to obtain CdSe QDs with the TOPO ligand (topoCdSe QDs). To study the effect of ligand substitution we also prepared CdSe QDs with pyridine surface ligand (pyrCdSe QDs). 10 vol % of pyridine was admixed to chloroform solution of topoCdSe QDs and kept for one week in dark.

2.2. Measurements and samples preparation

The morphology of the topoCdSe QDs (TOPO as the surfactant) was examined with a FEI Tecnai G² 20 X-TWIN Transmission Electron Microscope (TEM). For the TEM study a droplet of the topoCdSe QDs dispersed in chloroform was put onto TEM copper grid covered with ultrathin carbon (Ted Pella, Inc.) and allowed to dry. UV-VIS absorption spectra were recorded at room temperature with a Perkin Elmer Lambda 300 spectrophotometer.

Regioregular P3HT was purchased from Ossila Ltd. (electronic grade, RR = 96.6 %, M_w = 65 500 Da).

Chloroform solutions of P3HT (2 mg/ml, sonicated and heated to 50 °C to eliminate the

polymeric nanostructures in P3HT [26]) and of CdSe QDs (2 mg/ml) were mixed in various volume proportions to obtain P3HT:CdSe QDs mixtures with the mass ratios: 19:1, 9:1, 4:1 and 1:1 (only the results for two systems, 19:1 and 1:1, were chosen and discussed in this paper). As a reference, the neat solution of P3HT was used. As prepared solutions were used for film deposition by the spin coating method (at 900 rpm) in ambient air. Substrates (silicon wafers with deposited gold interdigital electrodes) were purchased from Fraunhofer Institut für Photonische Mikrosysteme (IPMS), Dresden. The thickness of SiO₂ layer was 230 nm, the gold electrodes were 30 nm thick (+ 10 nm ITO adhesion layer underneath). The width and length of the channel was 10 mm and 10 μm, respectively. The surface capacitance of the insulator was estimated to be 15 nF/cm². The schematic representation of the hybrid structure is shown in Fig. 3a. The output characteristics of OFETs were measured using a PC controlled system consisting of two Keithley 6517 electrometers. Charge carrier mobility (μ_{FET}) and threshold voltage (U_T) were determined within the saturation regime according to the following equation [27, 28]:

$$I_{SD} = \mu_{FET} \frac{WC}{2L} (U_{SG} - U_T)^2 \quad (1)$$

where I_{SD} is the source-drain current, U_{SG} is the gate voltage, C stands for insulator capacitance, W and L are the width and length of the channel, respectively. All measurements were performed in vacuum (< 3 Pa).

3. Results and discussion

Fig. 1a presents energy-dispersive X-ray (EDX) spectrum of the as-prepared CdSe QDs. The characteristic peaks of cadmium and selenium indicate that the obtained particles are indeed the CdSe compound. Additional peaks marked as P and Cu are due to copper and phosphor which come from the copper grid used in TEM sampling and the TOPO surfactant used during the synthesis of CdSe QDs, respectively. The chloroform dispersed CdSe QDs are uniform in

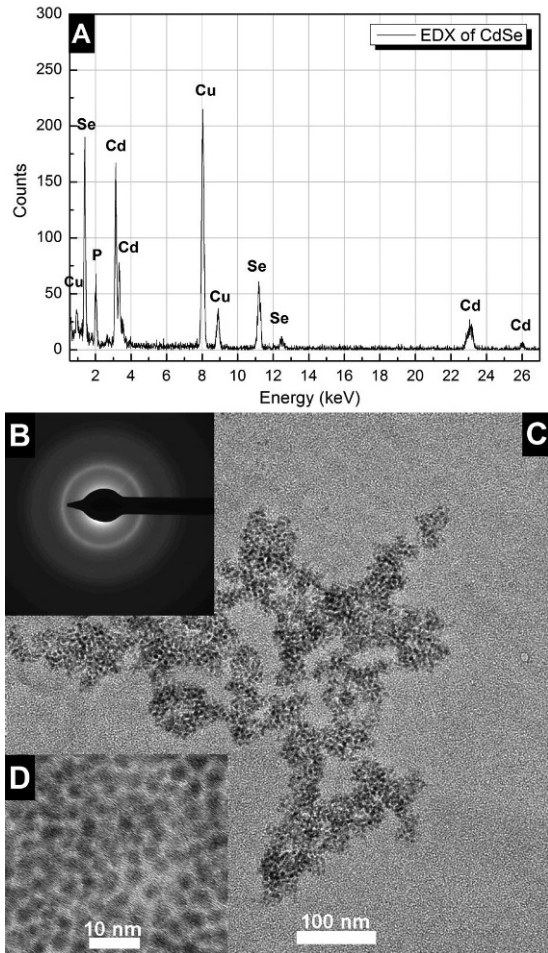


Fig. 1. Spectra of CdSe QDs: a) EDX, b) TEM, c) HRTEM and d) SAED micrographs of CdSe QDs showing the size uniformity of the dots.

size with a narrow size distribution, as shown by the TEM and high-resolution transmission electron microscopy (HRTEM) images (Fig. 1c, d). The average diameter of the dots is approximately 4 nm. The structure of the obtained materials was also proved by selected area electron diffraction (SAED).

Absorption spectra of chloroform solutions of CdSe QDs (with TOPO and pyridine as ligands) and the solid film of P3HT are shown in Fig. 2. The spectrum of P3HT chloroform solution shows a maximum at about 450 nm, the spectrum of the solid film is red shifted with maxima at 530 nm and 570 nm and one additional band at 610 nm [26]. The spectra of topoCdSe QDs and pyrCdSe QDs are nearly identical with a maximum at 600 nm.

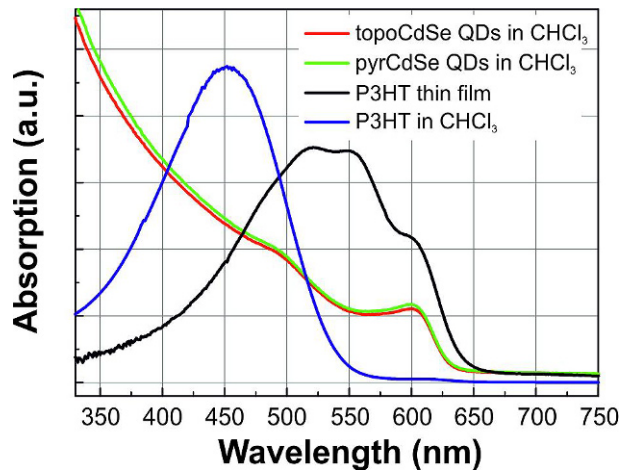


Fig. 2. UV-Vis absorbance spectra of topoCdSe QDs in chloroform, pyrCdSe QDs, P3HT in chloroform and P3HT thin film.

Output current-voltage characteristics of P3HT and P3HT:CdSe QDs FETs with TOPO and pyridine ligands are shown in Figs. 3b, 4 and 5. The basic parameters characterizing the charge transport are summarized in Table 1. The most interesting issue here is the influence of doping with the QDs on the value of the charge carrier mobility in the FET, μ_{FET} . In principle, one may expect that the presence of relatively low quantity of semiconductor particles in the polymer host may lead to formation of trapping states that reduce the value of the effective mobility. However, results reported in [18] indicate that, under some circumstances, the effect may be reverse, even at concentrations that are apparently too low to lead to percolation. The results of the present work are a bit perplexing. We found that the effective mobility in the P3HT:pyrCdSe QDs blend with mass ratio of 19:1 is practically the same as μ_{FET} in the undoped P3HT (Table 1, Fig. 6). On the other hand, μ_{FET} in the blend P3HT:topoCdSe QDs with mass ratio of 19:1 is one order of magnitude lower than the value of the mobility in undoped P3HT or P3HT:pyrCdSe QDs blend. Obviously, the influence of the QDs on the mobility depends critically on the type of the ligand present on the surface of the QDs. This can be construed to mean that in the case of topoCdSe in P3HT, quantum dot related trapping centers are formed while in the

case of pyrCdSe QDs no trapping is present or the effect of trapping is negligible.

To check the idea concerning trap formation due to the presence of QDs we determined the concentration of traps by calculating the subthreshold swing S parameter. This parameter represents the voltage swing required for a transistor to turn from off to on mode, and it should be as low as possible. In fact, high values of S are a drawback of organic transistors, resulting from a combination of low gate-dielectric capacitance, low breakdown voltage, and high parasitic capacitances at the insulator/semiconductor interface [29]. The maximum number of interface states N_t^{max} can be calculated using the relation [30]:

$$N_{Trap(max)} = \left[\frac{S \log(e)}{kT/q} - 1 \right] \frac{C}{q} \quad (2)$$

where C is the insulator capacitance, q is the elementary charge, T is the temperature, k is the Boltzmann constant and S is the subthreshold swing given by the expression:

$$S = \frac{dV_{GS}}{d \log(I_{DS})}. \quad (3)$$

The results obtained on the transistors described above are presented in Table 2. As expected, there are some differences between the densities of traps determined by this way, but they are not really concurrent with the changes in the effective mobility. Indeed, these results indicate approximately the same density of traps in the topoCdSe doped P3HT as in pristine polymer and a significantly lower trap density in the active layer in the case of the 19:1 mass ratio blend with pyrCdSe QDs. The results from Tables 1 and 2 can be discussed as follows. The concentrations of traps in P3HT and P3HT:topoCdSe QDs (19:1) are apparently the same but the charge carrier mobility in P3HT is by one order of magnitude higher than in the doped material. The measured mobility can be considered as an “effective” one and, in the case of band transport modulated by multiple trapping, can be written as $\mu = \theta \mu_o$, where μ_o is the trap-free mobility and the θ parameter is related to the

fraction of time that the carriers spend outside of traps when they actually take part in the conduction process. For monoenergetic traps it can be written as [31]:

$$\Theta = \frac{N_b}{N_t} \exp\left(-\frac{E_t}{kT}\right) \approx \frac{n_f}{n_f + n_t} \quad (4)$$

where N_b is the density of states, N_t is the concentration of traps, E_t is the trap depth, n_f is the free charge carrier concentration and n_t is the concentration of trapped charge carriers. The picture is more complicated in disordered molecular materials where the most probable transport mechanism is charge carrier hopping. The effective charge mobility in this case depends on the energetic distribution of the hopping states: the larger the distribution width, the lower the mobility [32]. If the trap concentration in both materials P3HT:topoCdSe QDs blend and P3HT is indeed the same (see Table 2) and the same trap depth is assumed, then the mobility decrease can be due to the energy broadening of the shallow transport hopping states. One needs to note that the concentration of traps determined using the value of subthreshold swing S refers to relatively deep traps close to the Fermi level.

To support the idea concerning the energy broadening of the hopping states we analyzed results obtained on samples with a high concentration of topoCdSe QDs in P3HT (1:1, see Fig. 7). As it follows from the figure, the transport in the blend has a much more dispersive character than that in pristine P3HT. A different situation is found for P3HT:pyrCdSe QDs blend. In this case, the effective charge carrier mobility in both materials (P3HT and P3HT:pyrCdSe QDs) is essentially the same but the trap concentration determined from the subthreshold swing is found to be lower in P3HT:pyrCdSe QDs blend than in pristine P3HT. However, the data in Fig. 7 indicate that for a high (1:1) concentration ratio of P3HT and pyrCdSe QDs the charge carrier transport is again dispersive. Thus, the broadening of the energetic distribution of the transport hopping states takes place also for the P3HT:pyrCdSe QDs system. A question arises why the trap concentration is lower. Several

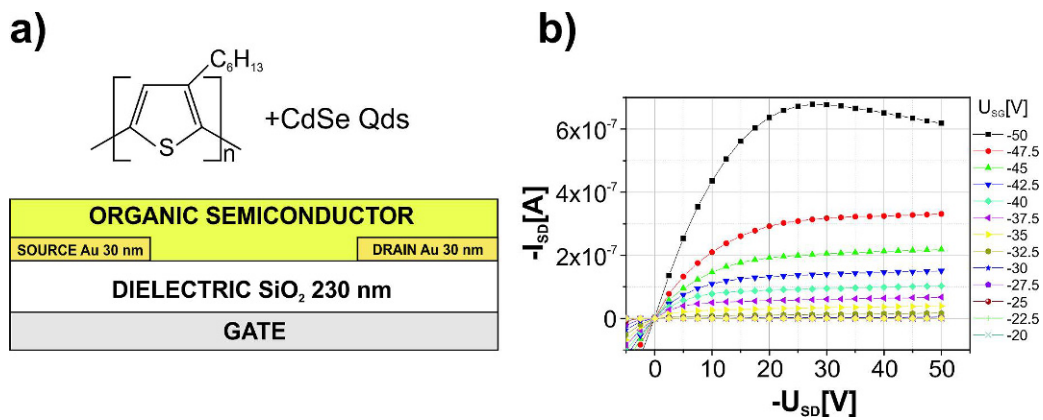


Fig. 3. Schematic representation of the FET hybrid structure (a). The chemical formula of P3HT and HRTEM of CdSe QDs (see Fig. 1) is given on the top of the scheme. An example of output current–voltage characteristics in P3HT OFET (b).

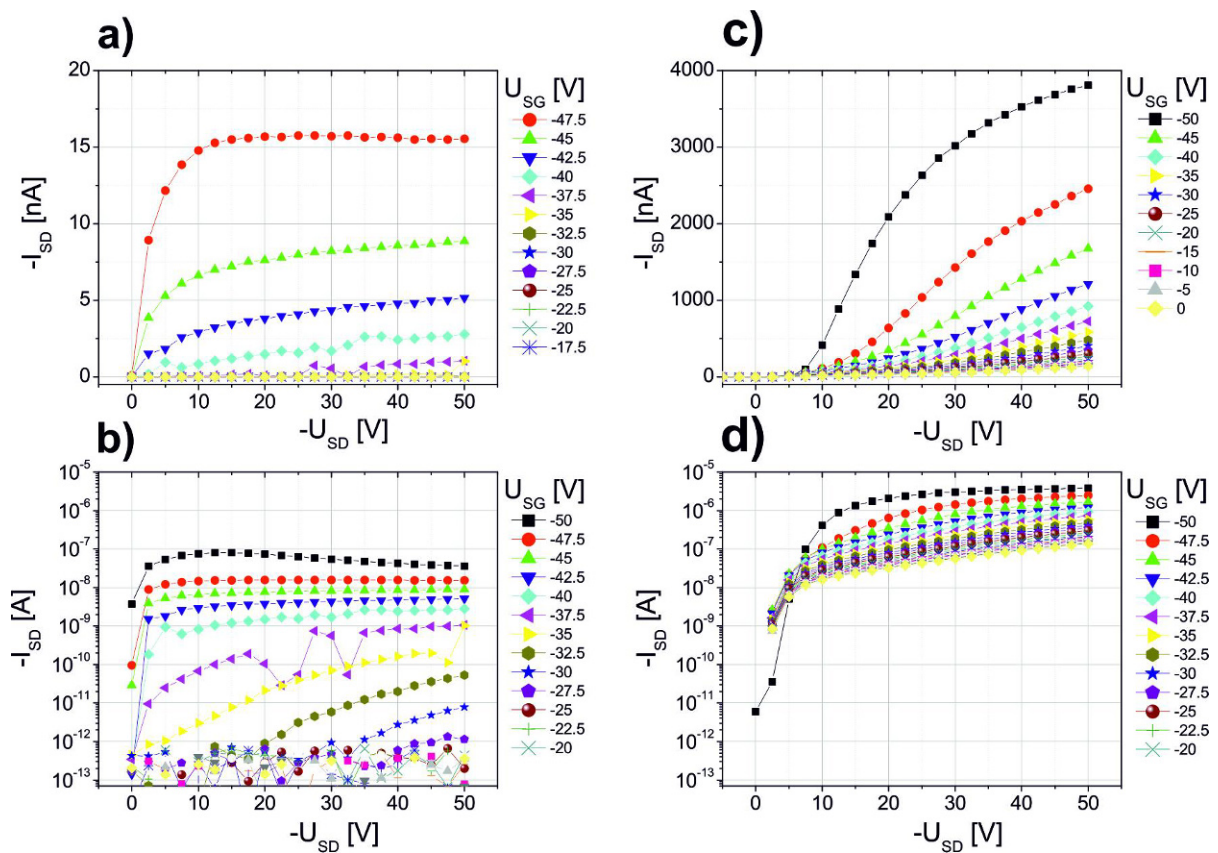


Fig. 4. Output current–voltage characteristics in P3HT doped topoCdSeQDs OFETs in linear (top) and in semilogarithmic scale (bottom) with P3HT:topoCdSe QDs mass ratio 19:1 (a, b) and 1:1 (c, d). Note the different scales of source-drain current in the diagrams.

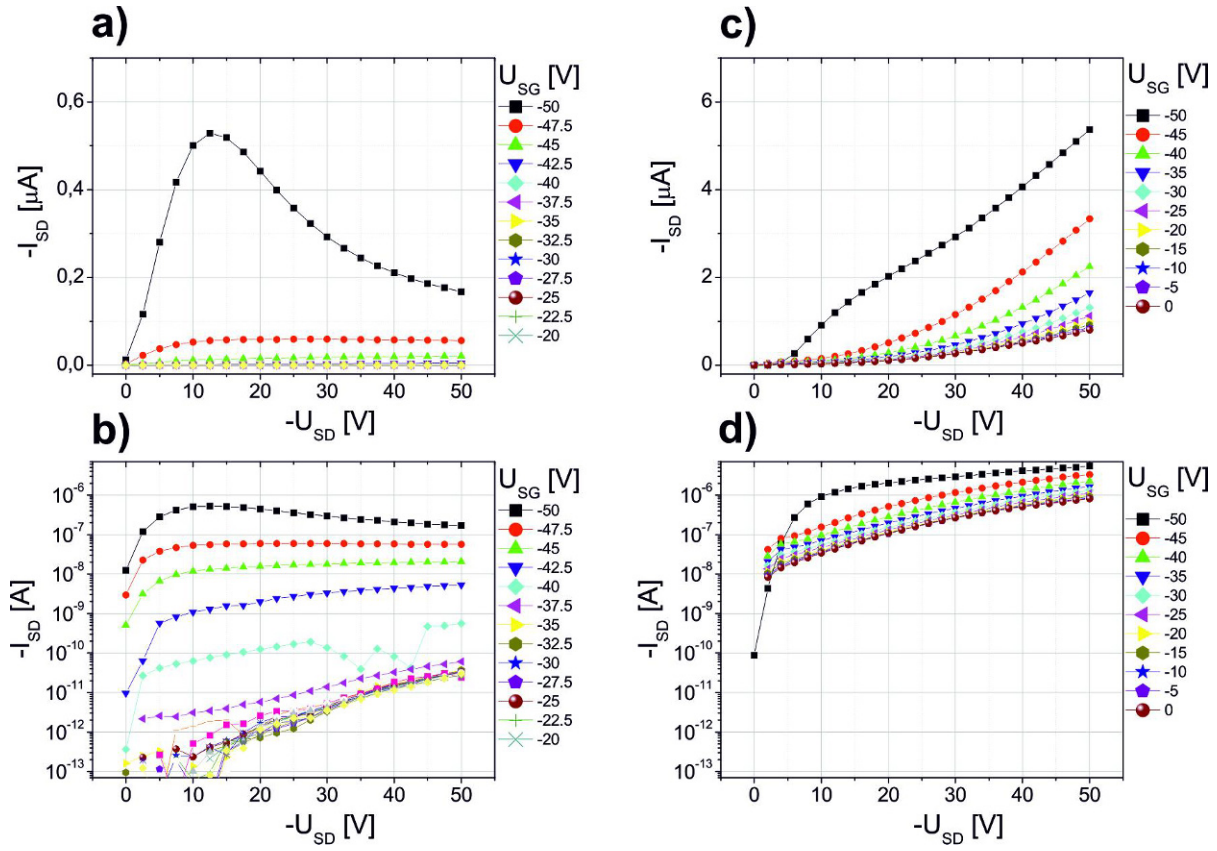


Fig. 5. Output current–voltage characteristics in P3HT doped pyrCdSe QDs OFETs in linear (top) and in semilogarithmic scale (bottom) with P3HT:pyrCdSeQDs mass ratio 19:1 (a, b) and 1:1 (c, d). Note the different scales of source-drain current in the diagrams.

Table 1. Average values of FET parameters.

	Reference	TOPO	Pyridine
P3HT:CdSe composition	1:0	19:1	19:1
Charge carrier mobility [cm^2/Vs] $\times 10^5$	11 ± 2	2 ± 1	11 ± 3
Threshold voltage [V]	28 ± 1	35 ± 1	38 ± 3
Δ Threshold voltage [V]	–	7.3	10.6
On/off	10^7	10^5	10^5
I_{DS} at $U_{GS} = -47.5\text{V}$; $U_{DS} = -45\text{V}$ [A]	3.5×10^{-7}	0.1×10^{-7}	0.5×10^{-7}

possibilities can be considered including formation of antitraps or destruction of some structural traps. One should also consider increasing the effective mobility through effects similar to those discussed in [18] where the increase of the mobility on doping with QDs was interpreted through the modification of the mean free path of

carriers. One should be careful, however, when comparing the mobility values obtained from the current-voltage characteristics of FETs to those from the time-of-flight measurements because the latter ones are obtained under conditions of only partial kinetic equilibrium that is established at

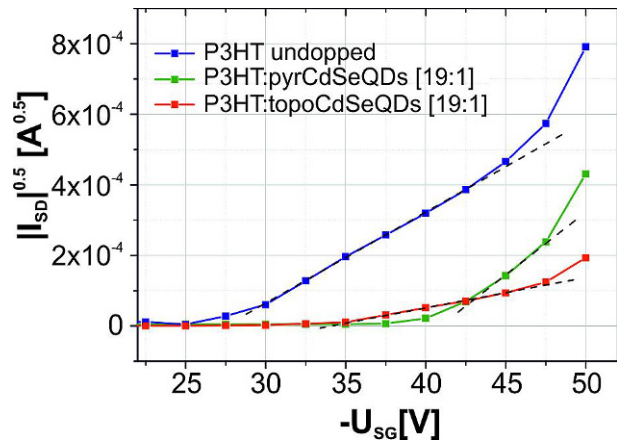


Fig. 6. Examples of transfer current–voltage characteristics of P3HT and P3HT doped CdSe QDs OFETs. The P3HT:CdSeQDs mass ratio 19:1 (see also Table 1).

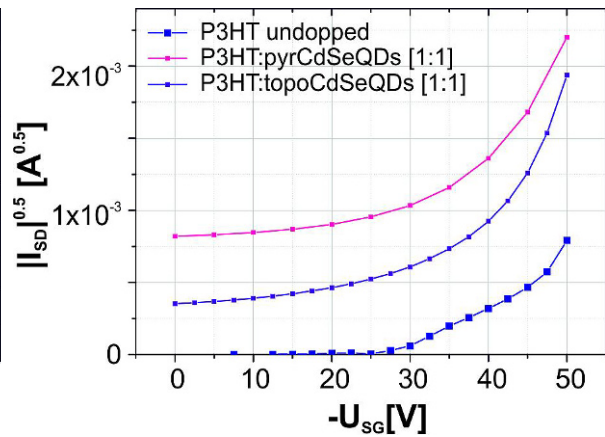


Fig. 7. Examples of transfer current–voltage characteristics of P3HT and P3HT doped CdSeQDs OFETs. The P3HT:CdSeQDs mass ratio 1:1.

Table 2. The comparison of the subthreshold swing and the maximal value of the density of interface trap states in the channel in P3HT:CdSe QDs based FETs.

	Reference	TOPO	Pyridine
P3HT:CdSe composition	1:0	19:1	19:1
S [V/decade]	5.5	5.3	2.6
$N_t^{(max)} \times 10^{12} [\text{cm}^{-2}]$	8.8	8.4	4.0

relatively short times during the transit of carriers through a thin film of a material.

Summarizing the experimental data for P3HT and the P3HT:pyrCdSe QDs blend: the mobilities appear to be the same, the concentration of traps and the on/off ratio are lower and the threshold voltage is higher in the P3HT:pyrCdSe QDs blend. In the case of antitrap formation (the possibility of the creation of these centers in organic materials was discussed for the first time in [21]) one can expect that the on/off ratio should decrease, which is in an agreement with our experimental results. On the other hand, the mobility is expected to increase – this is not observed in our experiment. However, one must be careful when discussing the electronic properties of an OFET device. The observed shift of the threshold voltage to higher negative values (see Table 1) could be connected

with the formation of a charge accumulation region at the source electrode [27]. Thus, our results might suggest that the addition of CdSe QDs to P3HT led to a higher voltage barrier at the electrode, irrespective of the surfactant. This can explain the decrease in I_{SD} in the case of P3HT:pyrCdSe QDs blend (cf. for example Figs. 3 and 5a,b; at $U_{SG} = -47.5$ V and $U_{SD} = -30$ V, the I_{SD} currents are -3×10^{-7} A and -5×10^{-8} A for P3HT and P3HT:pyrCdSe QDs blend, respectively). Another explanation might be the formation of a permanent electric field [24, 33].

Similar results concerning subthreshold swing were presented for FETs with ZnO particles [22]. It was shown that the presence of grains at the active layer/insulator interface decreases the defect density, especially at the grain boundary. In the system with large grains the number of grain boundaries and therefore the number of the gap and interface states is limited. This has a crucial influence on subthreshold swing and on the density of trap states [23]. In our case it might be suggested that larger nanostructures (grains) change the energy levels and the nanoparticles do not act as “anti-trapping” centers anymore. The HOMO level of a CdSe QD grain is close to the HOMO level of P3HT, the transport between P3HT and nanoparticle grains is easy and the active material shows the same hole mobility.

The antitrap formation was also discussed in blends of poly[2-methoxy-5-(2'-ethylhexyloxy)-p-phenylene vinylene]:zinc oxide nanocrystals (MEH-PPV:ZnO). Xu *et al.* [21] analyzed the energy diagrams and concluded that the main role of ZnO is to reduce the density of traps in the blend. Positive charge carriers are confined in the polymer matrix because of a huge energy barrier between MEH-PPV and ZnO valence bands (2.3 eV). Thus, ZnO forms "anti-trapping" centers. This results in the enhancement of MEH-PPV mobility. In our case we have not observed such a behavior.

The differences in the behavior of the QDs with the two types of ligands are quite significant. It is conventionally assumed that the surfactant used to protect the QDs should be chosen to minimize the distance between the host polymer matrix and the QDs and this should cause an easier exchange of charge carriers between the organic and inorganic components in the blend. This hypothesis was already discussed in literature, mainly in the context of solar cells *e.g.* [12, 34, 35]. But the role of trapping states due to the doping by QDs with different ligands is far from being clear. The ligands themselves should not act as trapping regions: the comparison of ionization potentials of a polythiophene chain, pyridine and the aliphatic 8-carbon chain of TOPO shows that it is impossible for the surfactants studied here to form chemical traps. On the other hand, it has been shown previously [8, 24] that ligands on the QD surface form barriers for electron tunneling into matrix. However, there are differences in the energy levels diagram between the two ligands [8]. *E.g.*, the difference between valence levels for nanoparticles with TOPO and pyridine as a ligand is *ca.* 0.3 eV [8, 24]. The important issue is of course that pyridine is a smaller molecule, which makes the electronic contact between P3HT and pyrCdSe QDs easier.

4. Conclusions

In summary, organic field effect transistors containing an active P3HT:CdSe QDs layer with various mass ratios were prepared and the effect of

the CdSe QDs capping ligand on their properties was investigated. In the case of mass ratio 19:1 the transfer characteristics showed that the charge carrier mobility can be only estimated. Incorporation of pyrCdSe QDs to the polymer matrix in a mass ratio 19:1 did not cause any changes in charge carrier mobility whereas the incorporation of topoCdSe QDs resulted in the decrease of this transport parameter. In both cases, the addition of topoCdSe QDs and pyrCdSe QDs into P3HT matrix caused the broadening of the energy distribution of transport hopping states. The increase of the additive concentration up to 1:1 made the charge transport fully dispersive. There are many factors which have to be taken into account for the explanation of the experimental data: (i) valence band energies of the matrix and components, (ii) structural disorder incorporated by the inorganic material, (iii) the density of traps and aggregation and (iv) the formation of anti-traps. In the case of pyridine as a ligand the process of the aggregation may play a critical role. However, the main conclusion from this work is that field effect transistor characteristics measurements do not provide an unequivocal answer to the question how the presence of QDs influences the transport properties of hybrid nanocomposites. One of the problems is that the FET parameters do not characterize only the active material but the whole device. Therefore, further investigations are needed where the FET measurements would be supplemented by space-charge-limited current and time-of-flight techniques.

Acknowledgements

This work was supported by the European Commission through the Human Potential Programme (Marie Curie RTN BIMORE, Grant No. MRTN-CT-2006-035859) and partially by a statutory activity subsidy from the Polish Ministry of Science and Higher Education for the Faculty of Chemistry of Wroclaw University of Technology. M.N. and M.S. acknowledge support from the Foundation for Polish Science (under the Welcome and Homing programs) and MNiSW Grant No. NN 507 599038. One of the authors (UB) is the recipient of the fellowship co-financed by European Union within European Social Fund.

References

- [1] BRAGA D., HOROWITZ G., *Adv. Mater.* 21/14-15 (2009), 1473.
- [2] WEN Y.G., LIU Y.Q., GUO Y.L., YU G., HU W.P., *Chem. Rev.* 111/5 (2011), 3358.
- [3] ORTIZ R.P., FACCHETTI A., MARKS T.J., *Chem. Rev.* 110/1 (2010) 205.
- [4] SALLES A., *Mater. Today* 10/3 (2007) 38.
- [5] KRUSZYNSKA M., KNIPPER M., KOLNY-OLESIK J., BORCHERT H., PARISI J., *Thin Solid Films* 519/21 (2011) 7374.
- [6] FARVA U., PARK C., *Sol. Energy Mater. Sol. Cells* 94/2 (2010) 303.
- [7] SHARMA S.N., KUMAR U., SINGH V.N., MEHTA B.R., KAKKAR R., *Thin Solid Films* 519/3 (2010) 1202.
- [8] ALDAKOV D., CHANDEZON F., DE BETIGNIES R., FIRON M., REISS P., PRON A., *Eur. Phys. J.-Appl. Phys* 36/3 (2006) 261.
- [9] CHOI H.J., YANG J.K., PARK H.H., *Thin Solid Films* 494/1-2 (2006) 207.
- [10] LIU I.S. et al., *J. Mater. Chem.* 18/6 (2008) 675.
- [11] SEO J., KIM W.J., KIM S.J., LEE K.S., CARTWRIGHT A.N., PRASAD P.N., *Appl. Phys. Lett.* 94/13 (2009) 133302.
- [12] LI Q.W., SUN B.Q., KINLOCH I.A., ZHI D., SIRRINGHAUS H., WINDLE A.H., *Chem. Mat.* 18/1 (2006) 164.
- [13] MILLIRON D.J., ALIVISATOS A.P., PITOIS C., EDDER C., FRECHET J.M.J., *Adv. Mater.* 15/1 (2003) 58.
- [14] HEINEMANN M.D. et al., *Adv. Funct. Mater.* 19/23 (2009) 3788.
- [15] CHOI S.H. et al., *J. Photochem. Photobiol. A-Chem.* 179/1-2 (2006) 135.
- [16] CHOI H.J., YANG J.K., YOON S., PARK H.H., *Appl. Surf. Sci.* 244/1-4 (2005) 92.
- [17] XU J. et al., *J. Am. Chem. Soc.* 129/42 (2007) 12828.
- [18] CHOUDHURY K.R., SAMOC M., PATRA A., PRASAD P.N., *J. Phys. Chem. B* 108/5 (2004) 1556.
- [19] NISHIOKA M., CHEN Y., GOLDMAN A.M., *Appl. Phys. Lett.* 92/15 (2008) 153308.
- [20] TOPP K. et al., *J. Phys. Chem. A* 114/11 (2010) 3981.
- [21] XU Z.X., ROY V.A.L., STALLINGA P., MUCCINI M., TOFFANIN S., XIANG H.F., CHE C.M., *Appl. Phys. Lett.* 90/22 (2007) 223509.
- [22] REMASHAN K., CHOI Y.S., PARK S.J., JANG J.H., *J. Electrochem. Soc.* 157/12 (2010) III121.
- [23] REMASHAN K., CHOI Y.S., PARK S.J., JANG J.H., *Jpn. J. Appl. Phys.* 50/4 (2011) 04DJ08.
- [24] CHIU M.Y., CHEN C.C., SHEU J.T., WEI K.H., *Org. Electron.* 10/5 (2009) 769.
- [25] NYK M., PALEWSKA K., KEPINSKI L., WILK K.A., STREK W., SAMOC M., *J. Lumines.* 130/12 (2010) 2487.
- [26] BIELECKA U., LUTSYK P., JANUS K., SWORAKOWSKI J., BARTKOWIAK W., *Org. Electron.* 12/11 (2011) 1768.
- [27] SZE S., NG K. (Eds.), *Physics of Semiconductor Devices*, Wiley & Sons Ltd., New York, 1997.
- [28] STALLINGA P. (Ed.), *Electrical Characterization of Organic Electronic Materials and Devices*, John Wiley & Sons Ltd., Chichester, UK, 2009.
- [29] XU W.T., RHEE S.W., *J. Mater. Chem.* 19/29 (2009) 5250.
- [30] NG K. (Ed.), *Complete guide to semiconductor devices*, John Wiley & Sons Ltd., New York, 2002.
- [31] SCHEINERT S., PAASCH G., SCHRODNER M., ROTH H.K., SENSFUSS S., DOLL T., *J. Appl. Phys.* 92/1 (2002) 330.
- [32] ARKHIPOV V.I., HEREMANS P., EMELIANOVA E.V., BASSLER H., *Phys. Rev. B* 71/4 (2005) 045214.
- [33] CHEN C.C., CHIU M.Y., SHEU J.T., WEI K.H., *Appl. Phys. Lett.* 92/14 (2008) 143105.
- [34] HUYNH W.U., DITTMER J.J., LIBBY W.C., WHITING G.L., ALIVISATOS A.P., *Adv. Funct. Mater.* 13/1 (2003) 73.
- [35] LEE H.J. et al., *J. Phys. Chem. C* 112/30 (2008) 11600.

Received 2012-08-30
Accepted 2013-02-26